

Michael Pfeiffer
Ulrich Boudriot
Dunja Pfeiffer
Natascha Ishaque
Werner Goetz
Axel Wilke

Intradiscal application of hyaluronic acid in the non-human primate lumbar spine: radiological results

Received: 27 October 2001
Revised: 8 April 2002
Accepted: 25 June 2002
Published online: 22 November 2002
© Springer-Verlag 2002

M. Pfeiffer (✉) · U. Boudriot · D. Pfeiffer
A. Wilke
Klinik für Orthopädie und Rheumatologie,
Philipps-Universität,
Baldingerstrasse,
35033 Marburg, Germany
e-mail:
michael.pfeiffer@med.uni-marburg.de,
Tel.: +49-6421-2864913,
Fax: +49-6421-2867007

N. Ishaque
Medizinisches Zentrum für Radiologie,
Klinik für Strahlendiagnostik,
Philipps-Universität, Marburg, Germany

W. Goetz
Anatomisches Institut,
Georg-August-Universität Göttingen,
Germany

Abstract Prospectively, with randomized segment-treatment assignment, and with blinded evaluators, lumbar motion segments in *Cercopithecus* monkeys were analyzed for macroscopic and radiological changes 24 weeks after nucleotomy and nucleotomy with additional intradiscal application of different hyaluronic acid formulations versus untreated control segments. The objective was to find out whether hyaluronic acid is able to influence the degenerative cascade in nonhuman primates after nucleotomy. In a similar procedure, hyaluronic acid has proven to decrease degeneration after nucleotomy in a Minipig model. This is the first such study ever undertaken in primates, thus trying to overcome the known limitations of non-primate spine models. Twenty monkeys with four segments each obtained nucleotomy in three segments and solely exposure of another control segment. Nucleotomy was performed from a transposoatic retroperitoneal approach. Preopera-

tive radiographs and follow-up radiographs, magnetic resonance imaging (MRI), computed tomography (CT), Q-CT with bone mineral density measurements and three-dimensional reconstruction were obtained and analyzed qualitatively and quantitatively. Segments with high-molecular-weight hyaluronic acid (Hylan G-F 20) application proved to be significantly superior over those with a standard nucleotomy in radiographs, MR images, CT scans, and macroscopic appearance at follow-up. Control segments remained unaffected. Interdependence between the different methods validated the utilized methods of quantitative radiological assessment of degeneration. Hylan G-F 20 appears to be a possible adjunct in reducing postoperative degeneration in an animal nucleotomy model. It deserves further evaluation, despite the fact that the mechanisms of its effects are still speculative.

Keywords Nucleotomy · Hyaluronic acid · Primates · Degeneration · In vivo

Introduction

Little is known about the possible enhancement of repair mechanisms of the functional spinal unit (FSU). Compared to other strategies in the treatment of degenerative disc disease (DDD), there has been little research in this field to date.

“Viscosupplementation” of other joints in the past has sparked great interest in both clinical and experimental

studies. Surprisingly, experimental results of hyaluronic acid (HA) application have so far gone almost unnoticed. HA as provided for therapeutic use [21] is similar to the indigenous hydrophilic component of the intervertebral extracellular matrix, meshing proteoglycans (PGs) and serving the structural integrity of the disc. In fresh disc herniation its concentration in the nucleus is allegedly increased, in contrast to chronic DDD [8, 9, 31].

To date, DDD, as manifested in disc prolapse/bulge and internal derangement, has yielded evidence for effi-

cacy of enhancement of intradiscal repair procedures in quadrupeds [17]. Evaluation of therapy in experimentally caused DDD relies on animal experiments. Only the lumbar FSU of primates consists of the same elements as in man (nucleus pulposus, annulus fibrosus, vertebral bodies and ligamentary structures) *without* the marked differences concerning the endplate regions in quadrupeds [6, 25].

After having established the general similarity of degeneration processes in a nucleotomy model in *Cercopithecus* with spontaneous DDD in humans [18], relations between macroscopic and radiological features should be characterized. Whether HA can slow down or prevent typical consecutive degenerative changes in comparison to standard nucleotomy and non-operated FSUs should be evaluated by means of an array of visualizing techniques.

Materials and methods

Animals

In a series of animal experiments in adult Green Vervet monkeys (*Cercopithecus aethiops*) we standardized the creation, evaluation, and classification of radiological phenomena in degenerative and reparative processes within the lumbar motion segment.

The average body mass for an adult male Vervet monkey is around 5 kg, and for a female about 3.5 kg. *Cercopithecus* moves predominantly quadrupedally both on the ground and in the trees, but also demonstrates so-called bipedal spy-hopping. In captivity it often stands upright without support of its arms or tail, or sits on its buttocks. Its lumbar spine (Fig. 1) consists of six to seven vertebrae with relatively broad transverse processes and neutral to slight lordotic lumbosacral angle.

Quarantined animals were provided by the Biomedical Research Centre, Pretoria, South Africa, where we were allowed to do the operations after obtaining consent from the Pretoria University Ethics Committee. After introducing anesthesia via Ketamine and Midazolam (i.m.), the animals, weighing between 3.0 and 6.6 kg, were shaved on their left flank. Two i.v. lines were placed



Fig. 1 Lateral (*right*) and anteroposterior radiographs of L3–L7 prior to operation. Note the slight lumbosacral lordosis and absence of degeneration

on the hindlegs, and radiographs taken in anteroposterior (AP) and lateral projection (64 mAs, 42 kV). The central beam was adjusted to the middle of the lumbar spine. Two animals with spine anomalies or pregnancy were excluded from the experiment. The remaining 20 animals (15 male, 5 female) were then intubated, and halothane inhalation administered. Pulse oxymetry, ECG monitoring, and fluid substitution were utilized.

The animals were placed in right lateral position on the operation table and, after sterile draping, a left longitudinal incision at the posterior parts of the M. obliquus externus was set. The latter was split, as were M. obliquus internus and M. transversus abdominis. A spreader was inserted, the retroperitoneal sac pushed aside and the psoas muscle visualized. In *Cercopithecus*, the psoas in relation to the vertebral bodies is somewhat wider than in man. Thus, we had to devise a novel transposoatic approach to the intervertebral spaces. At the posterior circumference of the vertebral bodies, nerve roots became visible and had to be protected. The genitofemoral nerve generally was circumvented.

Segment vessels were cauterized and three segments were nucleotomized in the following way: anterolateral cross incision of the annulus fibrosus with lancet #15 and insertion of a small forceps (as used in ear surgery), followed by localization of nucleus material and extraction without damaging the delicate cartilaginous endplates, and then final probing with a small curette without scraping.

At this point, in randomized assignment and order, now revealed to the surgeons from a list previously inaccessible to them, via a 22-G needle, one disc was refilled with ~0.5 ml commercially available Hylan G-F 20 with a molecular weight of 6×10^6 (Synvisc), one with the more viscous Hylan B of infinite molecular weight (Hylaform, both Biomatrix Inc., Ridgefield, USA), and one was left empty. Thus, the surgeons could not be blindfolded in respect of filling the disc, but were blinded for the foregoing preparation of the disc.

The annulus fibers were allowed to fold back, Hylan overflow was removed, and defects were sealed with small clots of fibrin glue (Tissucol Duo S, Baxter-Hyland-Immuno Division, Heidelberg, Germany), taking care that no glue was entering the disc space, but was merely covering the anterior longitudinal ligament. In the segments with nucleotomy alone, no fibrin glue was used. For re-identification of the segments, the middle vertebral body was marked with tantalum beads, which were inserted through a special impactor.

The animals were kept for 24–48 h postoperatively, caged in a recovery room under close supervision, after which they were moved to their usual cages and kept separately. Feeding was commenced again after 6–12 h. Buprenorphine was given i.m. 3 times/day for 2–3 days. A weight-adapted single-shot of second-generation cephalosporine was administered i.v. Immediately after awakening from intubation anesthesia, the sensibility and motoric response of the legs was tested (reflexes), wound checks were carried out regularly. Problems with stance and gait were monitored. Non-steroidal antiphlogistic substances were avoided. Any possible complication was noted and the possible need for operative re-intervention discussed.

The animals were sacrificed at 24 weeks follow-up time. After i.m. sedation with midazolam, the animals were X-rayed the same way as preoperatively. Thirty milliliters of 6% pentobarbital in 200 ml saline solution was administered i.v. before thoracotomy was carried out. A catheter system was inserted into the left heart ventricle for perfusion with 0.9% saline, the right ventricle was drained. After death, the entire lumbar spine was harvested, including parts of the sacrum, all paraspinous muscles, and the psoas compartment. The specimens were marked, vacuum sealed in plastic bags, fresh frozen at -80°C , and legally flown to Europe on dry ice for further analysis. Evaluating staff (U.B., W.G., D.P., N.I.), having been uninvolved in the experiment, were generally blindfolded in respect of treatment and segment assignment. All qualitative measurements were taken by two independent observers.

Injected materials

Hylans are derivatives of HA, consisting of repeated disaccharides of N-acetyl glucosamine and sodium glucuronate. Hylan G-F 20 (Synvisc) consists of a mix of Hylan A and Hylan B (8.0 mg/ml), in a buffer with a pH of 7.2. Hylan B (Hylaform) is provided in a concentration of 5.5 mg/ml suspended in buffer solution. It is provided in sterile disposable syringes of 2 ml and 0.5 ml respectively, and needs to be stored at between +2 and +30°C. It has viscoelastic properties and is hydrophilic.

Plain radiographs

The plain radiographs were digitized using a PC-linked VXR-12 Film Digitizer (Vidar Systems Corp., Freiburg, Germany) and DiagnostiX-32 V. 2.6.2 (GEMED, Freiburg, Germany). They were checked for signs of degeneration or adverse effects such as infection. Intervertebral distances of the three operated and one non-operated FSUs of each spine were determined, correcting for different magnification factors by relating to the sagittal diameter of the cranial vertebral body of the FSUs. Differences were calculated between the preoperative and follow-up distances. A comparable technique in man had shown an inter-observer error of 0.14 mm and a relative measurement error of 4.2% [4].

CT scans

Besides checking for signs of infection, spondylosis, osteochondrosis, and spondylarthritis (inter-observer correlation $r=1$, i.e. 100% concordance), CT and Q-CT analysis of the frozen specimens was done with a Siemens Somatom Plus 4, including three-dimensional reconstruction of selected specimens, on the basis of a Somaris-4 operating system (Siemens AG, Medical Solutions, Munich, Germany). Analysis of defined 2-mm-thick transverse regions of interest (ROI) of 0.1 cm² located at the mid portion of the vertebral body for bone mineral density (BMD) and at the middle of the disc for nucleus density, as calculated via Hounsfield units (HU), were related to a standard phantom, to warrant comparability among specimens by one observer. Additionally, differences between the operated and non-operated FSUs of the same spines were calculated. This latter quantitative assessment was done by one observer only.

MRI

After thawing of the specimens and suspension in a water bath, MRI was carried out as T1-SE (spin-echo, TR 540, TE 15), T2-TSE (turbo spin echo, TR 3500, TE 96) and DESS-3D (TR 28, TE 9) sequences with 1-mm slices on a 1-T Siemens Magnetom Expert with extremity coil, utilizing a Numaris-3 operating system (Siemens AG, Medical Solutions, Munich, Germany).

The obtained images – sagittal T1 and T2 (Fig. 2), sagittal and transverse DESS-3D – were analyzed with Osiris 4.0 (Digital Imaging Unit, University Hospital of Geneva): DESS-3D in respect of disc volume, T1 and T2 in respect of pixel values along a mid-sagittal center line through the disc. Differences between the operated and non-operated FSUs of the same spines were calculated.

T2 images were also graded according to Thompson et al. [23], scoring from grade 1 (absence of degeneration) to 5 (most severe degeneration), and checked for signs of spondylodiscitis according to Modic et al. [13] by two observers. The interobserver correlation for the Thompson grades was $r=0.939$, $P<0.001$, a maximum deviation of one grade was noted in 18%, no deviation in 82%. The ratings of extremes were always identical. In case of unequivocal assessment, both evaluators independently ranked the segment again and then chose a common assessment.



Fig. 2 Post-mortem sagittal T2-weighted magnetic resonance (MR) image of four segments with typical distribution of manipulation-dependent changes, showing marked degeneration at the lowest segment L7–S1 (standard nucleotomy), no degeneration in the topmost segment L4–5 (control segment), obvious degeneration with reduced nucleus signal, “fissures” extending in the annulus region, and signal intensity increase proximal and distal of the endplates at L5–6 (Hylan B). Segment L6–7 (Hylan G-F 20) preserves most similarities to the non-operated control

Macroscopic analysis

The analysis was based upon gross inspection of the thawed FSUs prior to and after mid-sagittal dissection for decalcification and histological analysis. The score utilized was developed upon the basis of other such scores [15, 17, 24], again ranging from 1 (absence of degeneration) to 5 (most severe degeneration). It is particularly suitable for sagittal or frontal sections, because the appearance of the endplates is incorporated into the score.

Statistical tools

A total of 80 FSUs could be used for explorative parametric and non-metric statistical analysis in this pilot study: ANOVA with post-hoc significance tests, calculation of linear correlation coefficients (“Pearson’s r ”), and the rank correlation test (“Spearman’s ρ ”). All criteria for test applicability were checked prior to calculation (e.g. tests for homogeneity of variances and normal distribution in parametric procedures). Significance level for the (two-tailed) tests was generally set to $P<0.05$. All these calculations were made in SPSS for Windows, v. 10.0.5. (SPSS Inc., Chicago, USA), after importing spreadsheets from Excel 2000 (Microsoft Corp., Redmond, USA).

Results

General results

All 20 *Cercopithecus* monkeys survived the full 24 weeks. Three complications occurred: two unilateral hind leg palsies and one wound dehiscence, which needed revision of the subcutaneous tissue. No obvious infection occurred. On average the animals lost 250 g of their body mass during that time.

All segments were unequivocally re-identified by comparing the operative notes with the tantalum bead placement on the final radiographs. Seventeen out of 20 animals had seven lumbar vertebrae, the remaining animals had six. The preoperatively planned equal level distribution for all the operative procedures was confirmed.

Plain radiographs

All FSUs prior to operation did not exhibit overt signs of degeneration (spondylosis, osteochondrosis, spondylarthritis), tumors, infections, and/or scoliosis.

The operated segments generally showed an average decrease of their intervertebral distance over the 24 weeks follow-up of between 12.4% and 34.6% of total disc space height in the lateral plane. The vertebral body height of all segments remained mostly unchanged, as did the intervertebral height of the control segments, thus indicating ab-

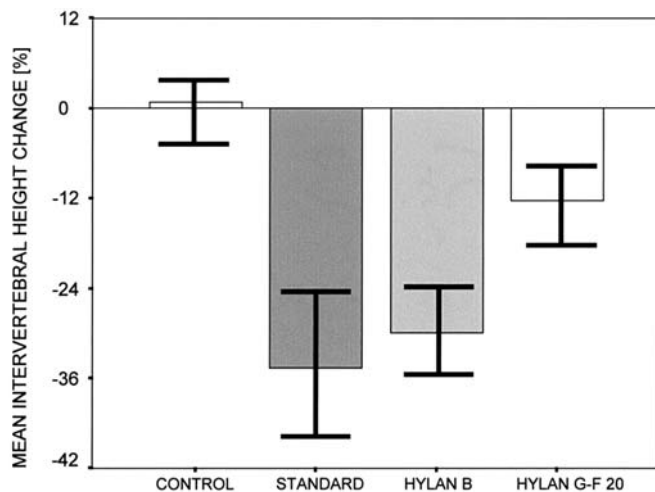


Fig. 3 The intervertebral height (all figures: mean values, 1 SD) is significantly reduced from beginning towards the end of the experiment in standard and Hylan B operated discs, whereas it remains virtually unchanged in the control segments: Hylan G-F 20 treated segments, on average, are the only ones whose height reduction, compared to untreated controls (left column), is insignificant, thus being significantly ($P < 0.026$) better than segments with nucleotomy only ("standard"). The difference between Hylan G-F 20 and Hylan B slightly missed significance ($P < 0.07$)

sence of adjacent segment degeneration above the operation levels.

Hylan G-F 20 kept the reduction of its segment height almost (about 10%) down to the level of non-operated control segments (which was significantly superior to the standard nucleotomy ($P < 0.026$)). Standard nucleotomy and Hylan B treated FSUs showed significantly more disc space narrowing than controls ($P < 0.001$ and $P < 0.003$ respectively, Fig. 3).

There was no spondylosis observed after Hylan G-F 20, Hylan B, and in control segments, whereas after standard nucleotomy spondylosis occurred in 10% ($P < 0.104$, n.s.).

There was one apparent fusion after standard nucleotomy and two after Hylan B, the first developing scoliosis. The reasons are yet to be clarified by histological analysis, since there had been no signs of infection detectable in the animals.

In a few cases, defects mimicking Schmorl's nodes were observed after nucleotomy.

CT scans

CT scans (Fig. 4) were more sensitive for detection of osteochondrosis and spondylosis than standard X-rays: six segments with osteochondrosis (7.5%) were found, half of which had undergone standard nucleotomy and half Hylan B application. There was no spondylosis except in standard nucleotomy segments. None of the facet joints exhibited severe spondylarthrosis, but the specimen size impeded a reliable grading of minor degenerative changes of these structures.

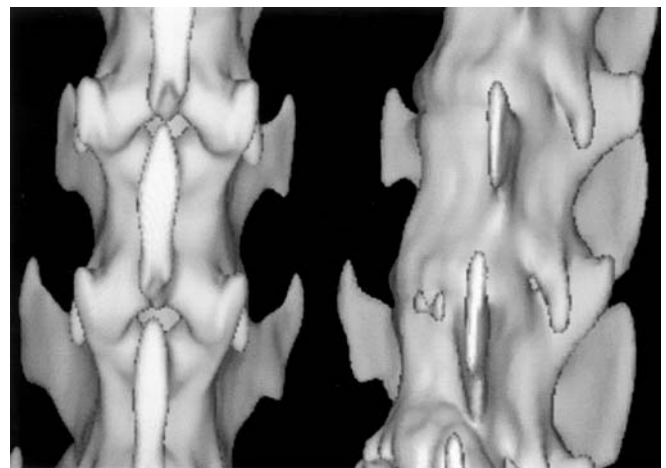


Fig. 4 On these three-dimensional computed tomography (CT) reconstructions (anterolateral oblique view on right, posterior on left side of the figure), a small double bony spur at the left anterolateral entrance is visualized between the transverse processes, which protrude slightly anterior (right side). Facet joints remain unaltered (left side of the picture). The anterolateral osteophyte had not been visible on standard radiographs

The nucleus density, quantified in Hounsfield units (HUs) of the regions of interest (ROIs) of the vertebral bodies and the intervertebral discs showed no significant differences for the different treatment modalities as compared to the control segments. HUs of the intervertebral disc, however, showed significantly increased inhomogeneity of the image (as characterized by its standard deviation, SD) with increasing loss of intervertebral height towards follow-up ($r=0.227$, $P<0.045$). Inhomogeneity was highest with standard nucleotomy.

MRI

At sacrifice, protrusions mimicking Schmorl's nodes, as well as some protruding into the spinal canal and anteriorly (but no complete or sequestered prolapses) were found on MRI. Entrance portals could sometimes be identified by ventral signal-rich areas on T1 images, but carried no resemblance to so-called high-intensity zones [14]. No intradiscal calcifications were detected on standard radiographs or on CT scans. There were no signs of spondylodiscitis or spondylitis in any of the segments according to Modic et al. [13].

A few lesions of the endplates were visualized best on the T2-weighted image. Bony spurs, osteophytes, and ossifications were difficult to find by means of MRI, which was inferior to CT and standard X-ray in detecting spondylosis.

For measuring the FSU height, standard X-rays were superior, because the margins of bony structures (e.g. at the cartilaginous endplate) are generally less well visualized on MRI.

Similar to human discs, healthy *Cercopithecus* discs showed a clearly distinct bright nucleus and dark black annulus area, especially on the T2-weighted image. The degenerated disc often displayed a dispersed dull white nucleus area and a more grayish annulus area without distinct borderlines or interspersed fissures (Fig. 2), resulting in a more homogeneous total appearance, with both significant increase of the midline mean T2 signal and reduction of its SD as compared to control segments.

Grading of the whole disc (T2) with the MRI degeneration score showed significantly fewer signs of degeneration with Hylan G-F 20 than with standard nucleotomy ($P<0.02$, Fig. 5). Compared to their controls, segments with high degeneration scores also had greater loss of intervertebral space height over time ($\rho=0.502$, $P<0.001$).

T1 signal alteration generally was less significant. Compared to their controls, Hylan-treated segments showed a trend towards mean signal increase, whereas after standard nucleotomy the mean signal intensity was somewhat reduced. The signal's SD tended to be increased in all operated segments.

Volume analysis showed that only Hylan G-F 20 treated discs, like non-operated discs, do not experience any vol-

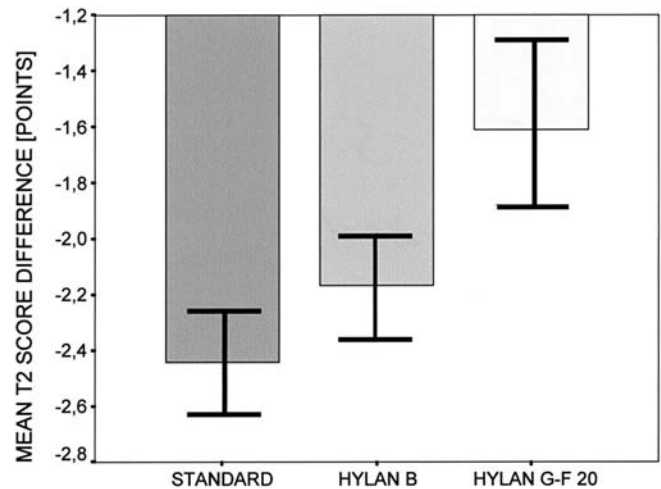


Fig. 5 Mean differences between T2 score and the score of the corresponding untreated control discs of the same spine: Hylan G-F 20 treated segments are significantly superior to standard nucleotomy discs ($P<0.02$)

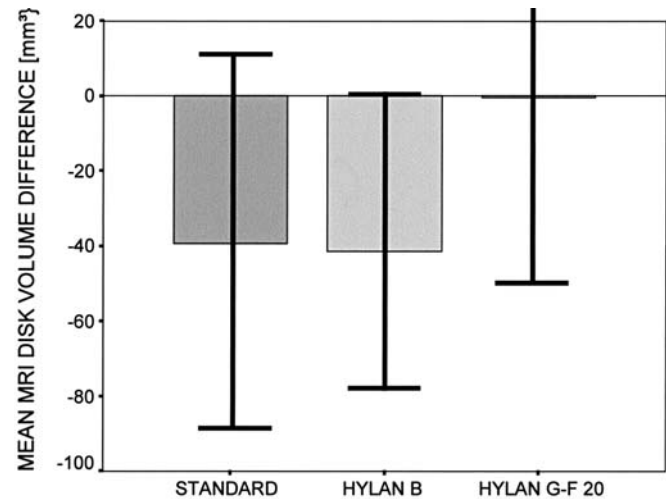


Fig. 6 The mean reduction of the operated disc's volume compared to their corresponding controls is around 40 mm³, except for Hylan G-F 20 treated discs, whose overall volume appears to be unchanged. However, high standard deviations call for a larger series to confirm the effect

ume reduction (Fig. 6). This was not for the price of anterior or posterior disc bulge or prolapse, which could lead to misinterpretation of volume measures: length ratio (MRI measured mid-sagittal disc diameter divided by the mid-sagittal diameter of the caudal vertebral body) of Hylan G-F 20 treated discs was not significantly different from all other segments.

High-volume discs also had a lower mean T1 signal than low-volume discs ($\rho=-0.404$, $P<0.002$) and a lower MRI degeneration score ($\rho=-0.359$, $P<0.01$).

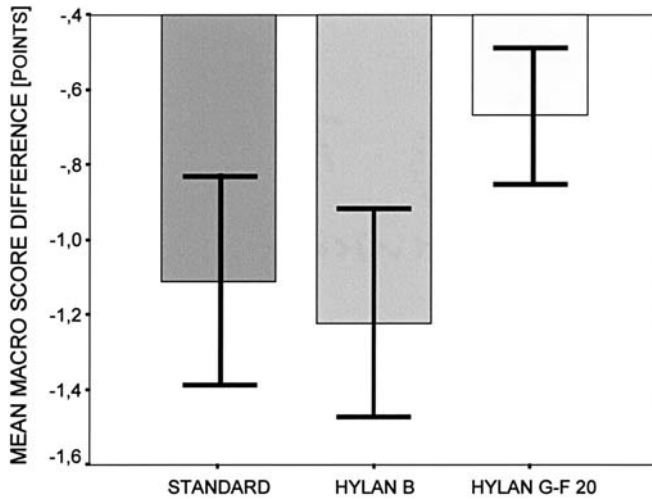


Fig. 7 The mean macroscopic score deterioration of the standard and Hylan B operated segments compared to their controls is more pronounced than in the case of Hylan G-F 20 treatment. Despite missing significance ($P < 0.10$), the difference between Hylan G-F 20 and the other segments is strikingly similar to Fig. 5 and Fig. 6

Macroscopic analysis

The full range of the macroscopic score was assigned during macroscopic analysis (Fig. 7). Non-operated segments had an average of 1.1 (min. 1, max 2), being significantly the best of all groups ($P_{\max} < 0.022$), standard nucleotomy yielded 2.28 (min. 1, max 5), Hylan B gave the same result as standard nucleotomy, and Hylan G-F 20 operated segments fared best of all with a mean of 1.78 (min. 1, max 4). Since a total of eight segments was unavailable for this examination, being used for biochemical analysis, Hylan G-F 20 slightly missed the significance limit in comparison to standard nucleotomy.

However, the macroscopic score closely reflects the results of the FSU height measurements on lateral radiographs. Related to the control segments of the same spine, intervertebral height difference over time and macroscopic score at sacrifice were correlated at $\rho = 0.356$, $P < 0.002$.

The same calculation with MRI grading yielded $\rho = 0.731$, $P < 0.001$ and with MRI disc volume resulted in $\rho = -0.301$, $P < 0.034$. With the inhomogeneity of the central disc ROI on CT scans, it was correlated at $\rho = 0.251$, $P < 0.035$.

Discussion

These intriguing results prompts one first to ask about the validity of the applied methods. Given the macroscopic inspection of a disc as a well-accepted method for assessment of degeneration, there was generally a significant intercorrelation between its results and specific lateral X-ray, transverse CT, and sagittal MRI parameters. These param-

eters, as mentioned above, can thus be recommended as valid tools for qualitative and quantitative assessment of disc degeneration, at least in the model presented.

Measuring degeneration scientifically, however, relies on standardized criteria, which can be obtained, among others, from macroscopic assessment and radiological methods. We had to accept that the *qualitative* analysis of radiographs and MR images [14, 27] is threatened by, for instance, high interobserver error [19, 27]. Qualitative analysis was generally carried out by two independent observers in our study.

Also, there is evidence that MRI, especially when *quantitative* methods are applied, does not only depict the disc matrix composition, but also the structural integrity of the matrix of the disc [1]. Signal intensity, however, is mathematically correlated with T1- and T2-relaxation times [28], which has often been the focus of quantitative MRI analysis.

The model itself has certain drawbacks: *Cercopithecus* is a relatively small animal, and a clinically practicable application of Hylans would have to utilize a *posterior* approach. This demand, in the meantime, has been fulfilled by a baboon model to be reported soon. Also, the discs were not actively pre-degenerated, i.e. the effects of the Hylans may not be transferable to already severely deteriorated discs without any potential left for self-repair.

Nevertheless, the basic mechanisms of disc degeneration could be mimicked by our blunt nucleotomy procedure. From previous results we know that simple annulus dissection without nucleotomy is not always sufficient for creating short-term degeneration in bigger animals such as sheep and pigs [16, 17].

It could be hypothesized from a previous study in Minipigs [17] that application of HA into the previously partially removed intervertebral disc leads to an improved and accelerated healing process, comprising of: an increased number of chondrocytes filling the defect, better preservation of intervertebral space height and mechanical properties of the FSU, absence of persistent necroses, and prevention of endplate lesions. Possibly, the applied HA forms a kind of lattice and stimulus for repair tissue activation. The proposed term “viscosupplementation” is probably not entirely adequate, because the applied HA, despite tight sealing with fibrin glue, will not prevail in the disc space for – at best – more than a few weeks, as can be concluded from current radioactive tracer studies. The tightness of the sealing can be proven by absence of any tracer leakage (data to be published).

HA is responsible for maintenance of the water-binding capacity of the disc and, thus, for preservation of its viscoelastic properties [21]. It is in therapeutic use in the spine for prevention of peridural adhesions [22], which makes it particularly alluring for future posterior use.

What are the possible mechanisms for the beneficial effects of Hylan G-F 20 that could be observed in our experiment?

It is known that in cartilage, with degeneration the PG synthesis and their binding sites for HA are diminishing. Since water content is correlated with the concentration of PGs [26, 30], viscoelasticity is thus reduced. Proteinases are generally held responsible for this phenomenon [12]. Decreased expression of these proteinases may be an effect of HA administration to cartilage cells [7], possibly by blocking cytokines. Release of body-own HA from chondrocytes is mediated by IL-1 and IGF-I [3], which is ubiquitous in complex interactive metabolic systems in the disc [5].

Lisignoli et al. [10], in a very recent paper, gave evidence that in cell cultures HA exerts an antiapoptotic effect on anti-FAS-induced chondrocyte apoptosis by binding its specific receptors (CD44 and ICAM-1). They conclude that HA may be able to slow down chondrocyte apoptosis by regulating the processes of cartilage matrix degradation.

Maldonado [11] found that only 15% of PGs synthesized by disc chondrocytes in cell cultures aggregate with HA. After administration of excess HA, 60% of the PGs are aggregating. This makes it clear that HA concentration plays a key role in the repair mechanisms of the disc.

Schleusener et al. [20] postulated chondroprotective and -proliferative effects of HA (after i.m. application) in a degeneration model in rabbit discs via inhibition of collagenase and increase of PG synthesis. A spacer function

until de-novo synthesis of HA by building of a fibrinogen-rich barrier against blood cells and fibrocytes seems to play an additional role in any local application [2].

Hylan G-F 20 (a mix of Hylan A and B) has rheological properties that come close to those of the intact nucleus pulposus. Pure Hylan B is more viscous. Both, at low concentrations, possess "pseudo-plastic" characteristics, i.e. subject to low shear forces, they exhibit a high viscosity, and under high shear forces a lower viscosity, because their molecular structure is load-dependent. A precondition for these effects in the disc is prevention of escape of the injected material. This can only be achieved by sealing the intradiscal cavity. Weigel et al. [29] showed specific interactions between HA and fibrinogen: fibrin polymerisation could be increased by 500% by application of only 60 μ M HA. Binding of HA worked with human and porcine fibrinogen. The thrombin-induced formation of fibrin clots is additionally increased and accelerated by HA. Even though Balasz and Denlinger rule out such an interaction for high-polymeric HA [2], this could be an explanation for the obviously tight sealing of the entrance portals with fibrin glue.

Acknowledgements The authors acknowledge Etienne Coetzee M.D., Jan Smuts, and Felipe Chaparro M. Med. Vet., Academic Hospital, Biomedical Research Centre, University of Pretoria, South Africa.

References

1. Antoniou J, Pike GB, Steffen T, Baramki H, Poole AR, Aebi M, Alini M (1998) Quantitative magnetic resonance imaging in the assessment of degenerative disc disease. *Magn Reson Med* 40:900–907
2. Balasz EA, Denlinger JL (1989) Clinical uses of hyaluronan. *Ciba Foundation Symposium*, 143:265–280
3. Fosang AJ, Tyler JA, Hardingham TE (1991) Effect of interleukin-1 and insulin like growth factor-I on the release of proteoglycan components and hyaluronan from pig articular cartilage in explant culture. *Matrix* 11:17–24
4. Frobin W, Brinckmann P, Biggemann M, Tillotson M, Burton K (1997) Precision measurement of disc height, vertebral height and sagittal plane displacement from lateral radiographic views of the lumbar spine. *Clin Biomech* 12[Suppl 1]:1–64
5. Götz W, Bertagnoli R, Herken R (1999) Struktur und Zusammensetzung der extrazellulären Matrix menschlicher Nuclei pulposi. In: Wilke HJ, Claes LE (eds) *Der Unfallchirurg*. Springer, Heidelberg Berlin, pp 3–15
6. Hansen H-J (1959) Comparative views on the pathology of disk degeneration in animals. *Lab Invest* 8:1242–1265
7. Kang Y, Eger W, Koepf H, Williams JM, Kuettner KE, Homandberg GA (1999) Hyaluronan suppresses fibronectin fragment-mediated damage to human cartilage explant cultures by enhancing proteoglycan synthesis. *J Orthop Res* 17:858–869
8. Kitano T, Zerwekh JE, Usui Y, Edwards ML, Flicker PL, Mooney V (1993) Biochemical changes associated with the symptomatic human intervertebral disk. *Clin Orthop* 293:372–377
9. Lipson SJ, Muir H (1981) Proteoglycans in experimental intervertebral disc degeneration. *Spine* 6:194–210
10. Lisignoli G, Grassi F, Zini N, Toneguzzi S, Piacentini A, Guidolin D, Bevilacqua C, Facchini A (2001) Anti-Fas-induced apoptosis in chondrocytes reduced by hyaluronan: evidence for CD44 and CD54 (intercellular adhesion molecule 1) involvement. *Arthritis Rheum* 44: 1800–1807
11. Maldonado BA (1990) Biosynthesis of proteoglycans by isolated intervertebral disc cells cultured in vitro. Transactions of the 36th Annual Orthopaedic Research Society Meeting, New Orleans, p 37
12. Melrose J, Ghosh P, Taylor TKF, Hall A, Osti OL, Vernon-Roberts B, Fraser RD (1992) A longitudinal study of the matrix changes induced in the intervertebral disc by surgical damage to the annulus fibrosus. *J Orthop Res* 10:665–676
13. Modic MT, Masaryk TJ, Ross JS, Carter JR (1988) Imaging of degenerative disk disease. *Radiology* 168:177–186
14. Morgan S, Saifuddin A (1999) MRI of the lumbar intervertebral disc. *Clin Radiol* 54:703–723
15. Nachemson A (1960) Lumbar intradiscal pressure: experimental studies on postmortem material. *Acta Orthop Scand Suppl* 43:62–74
16. Osti OL, Vernon-Roberts B, Fraser RD (1990) Annulus tears and intervertebral disc degeneration. An experimental study using an animal model. *Spine* 15: 762–767
17. Pfeiffer M, Griss P, Franke P, Bornscheuer C, Orth J, Wilke A, Clausen JD (1994) Degeneration model of the porcine lumbar motion segment: effects of various intradiscal procedures. *Eur Spine J* 3:8–16

18. Pfeiffer M, Wilke A, Goetz W, Chaparro F, Coetzee E, Griss P (2000) Comparison of two experimental models of intervertebral disc degeneration in mammals. *Transactions of the 11th Annual European Orthopaedic Research Society Meeting*, Wiesbaden, p 89
19. Raininko R, Manninen H, Battie MC, Gibbons LE, Gill K, Fisher LD (1995) Observer variability in the assessment of disc degeneration on magnetic resonance images of the lumbar and thoracic spine. *Spine* 20:1029–1035
20. Schleusener R, Schlegel J, Sawamura S, Edwards M (1991) Chondroproliferative effects of various agents on the degenerated rabbit intervertebral disc. Poster presentation at the 18th Annual International Society for Study of the Lumbar Spine Meeting, Heidelberg (available on request from corresponding author)
21. Scott JE (1989) Secondary structures in hyaluronan solutions – chemical and biological implications. *Ciba Foundation Symposium* 143:6–20
22. Songer MN, Ghosh L, Spencer DL (1990) Effects of sodium hyaluronate on peridural fibrosis after lumbar laminotomy and discectomy. *Spine* 15:551–554
23. Thompson JP, Pearce RH, Ho B (1988) Correlation of gross morphology and chemical composition with magnetic resonance images of human intervertebral discs. *Trans Orthop Res Soc* 13: 276–283
24. Thompson JP, Pearce RH, Schechter MT, Adams ME, Tsang IK, Bishop PB (1990) Preliminary evaluation of a scheme for grading the gross morphology of the human intervertebral disc. *Spine* 15:411–415
25. Töndury G (1958) Allgemeine Entwicklungsgeschichte der Wirbelsäule – Verknöcherung der Wirbel – Der Verknöcherungsprozeß nach der Geburt. In: Junghans W (ed) *Entwicklungsgeschichte und Fehlbildungen der Wirbelsäule*. Hippokrates, Stuttgart, pp 46–55
26. Urban JPG, McMullin JF (1988) Swelling pressure of the lumbar intervertebral discs: influence of age, spinal level, composition, and degeneration. *Spine* 13:179–187
27. Videman T, Battie MC, Gill K, Manninen H, Gibbons LE, Fisher LD (1995) Magnetic resonance imaging findings and their relationships in the thoracic and lumbar spine. Insights into the etiopathogenesis of spinal degeneration. *Spine* 20:928–935
28. Weidenbaum M, Foster RJ, Best BA, Saed-Neja F, Nickoloff E, Newhouse J, Ratcliffe A (1992) Correlating magnetic resonance imaging with the biochemical content of the normal human intervertebral disc. *J Orthop Res* 10: 552–561
29. Weigel PH, Frost SJ, LeBeoeuf RD, McGary CT (1989) The specific interaction between fibrin(ogen) and hyaluronan: possible consequences in haemostasis, inflammation and wound healing. *Ciba Foundation Symposium* 143:248–264
30. Ziv I (1990) The relationship between the degeneration of the human intervertebral disc and facet joints of the same lumbar segment – a physico chemical study. *Transactions of the 36th Annual Orthopaedic Research Society Meeting*, New Orleans, p 599
31. Zöllner J, Sancaktaroglu T, Meurer A, Grimm W, Andreas J, Eysel P (1999) Bestimmung der Hyaluronsäure im Nucleus pulposus bei akuten und chronisch degenerativen Bandscheibenveränderungen. *Z Orthop* 137:211–213